JOURNAL OF VIROLOGY, Apr. 1999, p. 2963–2973 Vol. 73, No. 4
0022-538X/99/$04.00+0

Reovirus Virion-Like Particles Obtained by Recoating Infectious Subvirion Particles with Baculovirus-Expressed σ3 Protein: an Approach for Analyzing σ3 Functions during Virus Entry

JUDIT JANÉ-VALBUENA,[1,2] MAX L. NIBERT,[1,2]* STEPHAN M. SPENCER,[1,2] STEPHEN B. WALKER,[3] TIMOTHY S. BAKER,[3] YA CHEN,[4] VICTORIA E. CENTONZE,[4] AND LESLIE A. SCHIFF[5]

Department of Biochemistry, College of Agricultural and Life Sciences,[1] and Institute for Molecular Virology[2] and Integrated Microscopy Resource,[4] The Graduate School, University of Wisconsin—Madison, Madison, Wisconsin 53706; Department of Biological Sciences, Purdue University, West Lafayette, Indiana 47907[3]; and Department of Microbiology, University of Minnesota Medical School, Minneapolis, Minnesota 55455[5]

Received 20 August 1998/Accepted 8 December 1998

Structure-function studies with mammalian reoviruses have been limited by the lack of a reverse-genetic system for engineering mutations into the viral genome. To circumvent this limitation in a partial way for the major outer-capsid protein σ3, we obtained in vitro assembly of large numbers of virion-like particles by binding baculovirus-expressed σ3 protein to infectious subvirion particles (ISVPs) that lack σ3. A level of σ3 binding approaching 100% of that in native virions was routinely achieved. The σ3 coat in these recoated ISVPs (rcISVPs) appeared very similar to that in virions by electron microscopy and three-dimensional image reconstruction. rcISVPs retained full infectivity in murine L cells, allowing their use to study σ3 functions in virus entry. Upon infection, rcISVPs behaved identically to virions in showing an extended lag phase prior to exponential growth and in being inhibited from entering cells by either the weak base NH_4Cl or the cysteine proteinase inhibitor E-64. rcISVPs also mimicked virions in being incapable of in vitro activation to mediate lysis of erythrocytes and transcription of the viral mRNAs. Last, rcISVPs behaved like virions in showing minor loss of infectivity at 52°C. Since rcISVPs contain virion-like levels of σ3 but contain outer-capsid protein μ1/μ1C mostly cleaved at the δ-ϕ junction as in ISVPs, the fact that rcISVPs behaved like virions (and not ISVPs) in all of the assays that we performed suggests that σ3, and not the δ-ϕ cleavage of μ1/μ1C, determines the observed differences in behavior between virions and ISVPs. To demonstrate the applicability of rcISVPs for genetic studies of protein functions in reovirus entry (an approach that we call recoating genetics), we used chimeric σ3 proteins to localize the primary determinants of a strain-dependent difference in σ3 cleavage rate to a carboxy-terminal region of the ISVP-bound protein.

Mammalian orthoreoviruses (reoviruses) serve as useful models to study the viral and cellular determinants that enable nonenveloped viruses to enter cells and initiate infection. The mature reovirus virion comprises two concentric icosahedral capsids, which in turn surround the segmented double-stranded RNA genome. Outer-capsid proteins σ1, σ3, and μ1/μ1C play critical roles in virus entry. The first step in entry, binding to cell surface receptors, is mediated by the σ1 trimer located at each fivefold axis in virions (24, 26, 49). Following receptor binding, reovirus virions are delivered into endocytic compartments, where they undergo partial uncoating. By this process the major outer-capsid proteins σ3 and μ1/μ1C, present in 600 copies each, are proteolytically cleaved, yielding subvirion particles (16, 48) with similarities to the infectious subvirion particles (ISVPs) that can be generated by in vitro proteolysis (7, 30, 45). Notable features of these subvirion particles include loss of σ3 and cleavage of μ1/μ1C within a defined region near its C terminus to generate particle-bound fragments μ1δ/δ and ϕ (40). Subsequent to the required cleavages of σ3 and/or μ1/μ1C, the μ1/μ1C protein is thought to undergo a change in conformation analogous to those by the fusion proteins of enveloped viruses, giving it the capacity to perturb the integrity of the adjacent membrane bilayer (9, 14, 15, 27, 35, 39, 52). This interaction provides access to the cytoplasm for the resulting subvirion particle in which the particle-associated enzymes for transcription of the viral mRNAs are activated from their latent state in virions (8, 10, 14, 19, 22, 30, 45).

Although proteolysis of outer-capsid proteins is essential for productive infections (see below), the molecular basis for this requirement remains to be fully characterized. In nature, reoviruses infect via the enteric and respiratory tracts. Studies with proteinase inhibitors have shown that in the intestinal tract, proteolysis of outer-capsid proteins by pancreatic serine proteinases, generating ISVP-like subvirion particles, is required for at least some reovirus strains to adhere to M cells and infect intestinal target tissues (1, 6). In contrast, when reoviruses infect via the respiratory tract, where the concentration of extracellular proteinases is low, proteolysis more likely occurs after uptake of virions into the acidic endocytotic compartments of target cells. Studies with cultured cell lines have clearly demonstrated the need for intracellular proteolysis during infections with intact reovirus virions. In culture, infections with virions, but not ISVPs, can be blocked by treating cells with weak bases like NH_4^+ (e.g., from NH_4Cl) that raise pH in acidic compartments in cells, including endosomes and lysosomes (3, 12, 50). Similar results are obtained with E-64, an inhibitor of papain family cysteine proteinases, including several that reside in mammalian lysosomes (3, 15). Treatment with pepstatin A, an inhibitor of aspartic proteinases including cathepsin D in mammalian lysosomes, however, has no effect

* Corresponding author. Mailing address: Institute for Molecular Virology, University of Wisconsin—Madison, 1525 Linden Dr., Madison, WI 53706. Phone: (608) 262-4536. Fax: (608) 262-7414. E-mail: mlnibert@facstaff.wisc.edu.

on reovirus infections (32). Together, these data indicate that specific cellular proteinases participate in cleaving σ3 and/or μ1/μ1C during entry into cells. Recent evidence indicates that the effects of E-64 and NH_4Cl on reovirus infections can be overcome by infecting cells either with ISVPs (3, 50) or with dpSVPs, distinct subvirion particles which are like ISVPs in lacking σ3 but like virions in having very few μ1/μ1C molecules cleaved at the δ-ϕ junction (15). The latter finding suggests that cleavage of μ1/μ1C at the δ-ϕ junction during reovirus entry is dispensable for infection and that only cleavages of σ3 are required. Many molecular details of reovirus entry, including which cleavages of σ3 are needed to activate the membrane-disrupting potential of the underlying μ1/μ1C protein and which host proteinases effect these cleavages, remain to be determined.

To understand the molecular basis of reovirus entry in greater detail, we sought to develop a system in which the σ3 protein could be altered (e.g., by site-directed mutagenesis) and assembled into virion-like particles, after which the consequences of these mutations on virion structure and entry into cells could be analyzed. Chang and Zweerink (16) provided the first evidence that σ3 protein derived from reovirus-infected L cells can bind to ISVP-like subvirion particles generated during reovirus infection. Subsequent studies by Astell et al. (2) showed that the reassembled particles obtained in this manner are similar to native virions in density, appearance in electron micrographs, and insensitivity to transcriptase activation. Recent work in one of our laboratories showed that σ3 generated by in vitro transcription-translation, using a σ3-encoding S4 cDNA (31), can bind to purified ISVPs and remain bound through purification in a CsCl gradient (46). Moreover, the conformation of the σ3 molecules bound to ISVPs appeared identical to that bound to virions, based on an identical pattern of σ3 cleavage fragments following limited in vitro digestion with proteinase K (46).

Although in vitro transcription-translation generates sufficient amounts of σ3 for many types of analytical studies with recoated particles (46), that approach is not conducive to obtaining large numbers of virion-like particles. Here, we demonstrate that this limitation can be overcome by using σ3 protein from lysates of insect cells that are infected with a recombinant baculovirus providing high levels of σ3 expression. Using baculovirus-expressed σ3 protein, we approximated stoichiometric recoating of large numbers of ISVPs and performed studies which indicate that these recoated ISVPs (rcISVPs) mimic both the appearance and the behavior of virions in several respects. We conclude from these studies that σ3, and not the δ-ϕ cleavage of μ1/μ1C, is the primary determinant of structural and functional differences between virions and ISVPs. Since virion-like particles can be similarly reconstituted with σ3 mutants (29), we can now explore the roles of σ3 in reovirus entry by using an approach that we call recoating genetics. To demonstrate this approach, we used chimeric σ3 proteins to localize the primary determinants of a strain-dependent difference in σ3 cleavage rate to a C-terminal region of the ISVP-bound protein.

MATERIALS AND METHODS

Cells. Spinner-adapted L cells were grown in Joklik's modified minimal essential medium (Irvine Scientific Co., Irvine, Calif.) supplemented to contain 2% fetal bovine serum, 2% neonatal bovine serum (HyClone Laboratories, Logan, Utah), 2 mM glutamine, 100 U of penicillin per ml, and 100 μg of streptomycin per ml (Irvine Scientific). *Spodoptera frugiperda* clone 21 (Sf21) insect cells (Invitrogen, Carlsbad, Calif.) were grown in TC-100 medium (Gibco BRL, Gaithersburg, Md.) supplemented to contain 10% heat-inactivated fetal bovine serum.

Recombinant baculovirus containing the reovirus T3D S4 gene. A cDNA copy of the reovirus type 3 Dearing (T3D) S4 gene (31) was subcloned into the *Eco*RI site of the transfer plasmid pEV/35K/ polybsmcr (34) under transcriptional control of the baculovirus polyhedrin promoter. Recombinant baculoviruses containing the polyhedrin-S4 construct (termed S4D-baculoviruses) were then obtained and amplified as described for the reovirus S3 gene (25). Expression of the T3D σ3 protein upon infection of Sf21 cells with S4D-baculoviruses was confirmed by sodium dodecyl sulfate (SDS)-polyacrylamide gel electrophoresis (PAGE) and immunoblotting.

Expression of σ3 in insect cells. Sf21 cells (5×10^6) were infected with S4D-baculovirus at 10 PFU/cell. Cells were harvested at 48 h postinfection, washed with phosphate-buffered saline (PBS: 137 mM NaCl, 8.1 mM Na_2HPO_4, 2.7 mM KCl, 1.5 mM KH_2PO_4 [pH 7.5]), and lysed with 800 μl of lysis buffer (20 mM Tris, 5 mM $MgCl_2$, 1% Triton X-100, 0.1 M NaCl, 5 μg of leupeptin per ml, 1 mM phenylmethylsulfonyl fluoride [pH 7.4]) by incubation on ice for 30 min. Immediately after incubation, the lysed cells were pelleted by centrifugation at $500 \times g$ for 10 min at 4°C. The soluble (cytoplasmic) fraction was removed, and the pellet was resuspended in 800 μl of PBS adjusted to contain 500 mM NaCl. After centrifugation at $22,000 \times g$ for 10 min, the new soluble fraction (nuclear lysate), which contained most of the σ3 protein, was harvested.

Virions and ISVPs. Virions of reovirus type 1 Lang (T1L) or T3D were obtained by the standard protocol (24) and stored in virion buffer (150 mM NaCl, 10 mM $MgCl_2$, 10 mM Tris [pH 7.5]). To obtain T1L ISVPs, the same protocol was followed except that after the second freon extraction, virions were diluted in virion buffer and pelleted by centrifugation at 5°C in an SW28 rotor (Beckman Instruments, Palo Alto, Calif.) spun at 25,000 rpm for 2 h. The pelleted virions were resuspended in virion buffer at a concentration lower than 10^{13} particles/ml and treated with 200 μg of *N*α-*p*-tosyl-L-lysine chloromethyl ketone (TLCK)-treated α-chymotrypsin (CHT) (Sigma Chemical Co., St. Louis, Mo.) per ml for 50 min at 37°C. ISVPs were purified by centrifugation in a preformed CsCl gradient (24) and stored in virion buffer after dialysis. All particle concentrations were determined from A_{260} (17).

rcISVPs. Purified T1L ISVPs were incubated at room temperature for 30 min with nuclear lysate derived from Sf21 cells infected with S4D-baculovirus. Stoichiometric recoating was routinely achieved by adding lysate from 5×10^6 infected cells to 2.5×10^{12} ISVPs. Virion buffer was added to decrease the NaCl concentration of the final mixture to 250 to 350 mM. Immediately after incubation, the sample was layered on a preformed CsCl density gradient (1.27 to 1.46 g/cm^3) and subjected to centrifugation at 5°C in an SW41 rotor (Beckman) spun at 35,000 rpm for at least 4 h. The particle band was harvested and dialyzed into virion buffer. Particle concentration was determined from A_{260} values, using the conversion factor corresponding to virions (17).

SDS-PAGE and immunoblotting. Samples to be analyzed by SDS-PAGE were diluted 2:1 with 3× sample buffer (375 mM Tris, 30% sucrose, 3% SDS, 6% β-mercaptoethanol, 0.03% bromophenol blue [pH 8.0]) and boiled for 1 to 2 min. Ten percent acrylamide gels were used, and proteins were visualized by staining with Coomassie brilliant blue R-250 (Sigma). For immunoblots, protein samples were subjected to SDS-PAGE and transferred to nitrocellulose at 4°C overnight at 30 V in transfer buffer (25 mM Tris, 192 mM glycine, 20% methanol [pH 8.3]). Mouse-derived, σ3-specific monoclonal antibody 4F2 (53) was used at a 1/2,000 dilution of a 1-mg/ml stock. Detection of this antibody was achieved by using 1/3,000 alkaline phosphatase-coupled goat anti-mouse immunoglobulin (Bio-Rad Laboratories, Hercules, Calif.) with 300 μg of *p*-nitroblue tetrazolium chloride per ml and 150 μg of 5-bromo-4-chloro-3-indolyl phosphate *p*-toluidine per ml (Bio-Rad) in substrate buffer (100 mM Tris, 0.5 mM $MgCl_2$ [pH 9.5]).

Buoyant densities. Particles (2×10^{11}) were layered on a 10-ml 1.30- to 1.46-g/cm^3 preformed CsCl gradient and subjected to centrifugation at 5°C in an SW41 rotor (Beckman) spun at 25,000 rpm for 12 to 16 h. Gradients were fractionated into 300-μl aliquots by collection from bottom to top, using a peristaltic pump (Rainin Instrument Co., Woburn, Mass.). Fractions containing virus particles were located by measuring A_{260}, and buoyant densities of the peak fractions were determined by measuring refractive indices with a digital refractometer (Bausch & Lomb, Rochester, N.Y.).

Electron microscopy and 3-D image reconstruction. Fresh rcISVPs samples were prepared for conventional transmission electron microscopy (TEM) as described previously (13). Samples of freshly generated rcISVPs were prepared for low-temperature, high-resolution scanning electron microscopy (cryo-SEM) and viewed as described previously (13). Images were acquired in digital format directly from the microscope by using Digital Micrograph (Gatan), and their brightness and contrast were optimized by using Photoshop (Adobe Systems, Mountain View, Calif.). For low-temperature, high-resolution TEM (cryo-TEM), purified rcISVPs were embedded in vitreous ice, and micrographs were recorded at a nominal magnification of ×38,000, using standard low-dose cryo-TEM procedures on a Philips CM200 microscope (5). Ninety-one particles were selected from three micrographs (defocus values of 2.1, 2.6, and 3.3 μm) and analyzed with image processing techniques for icosahedral particles (4, 23). The particle orientations were evenly distributed throughout the asymmetric unit, as evidenced by all inverse eigenvalues being <1.0 and at least 99% being <0.1 (23). The final three-dimensional (3-D) reconstruction was calculated at 33-Å resolution.

Plaque assays. Plaque assays to determine particle/PFU ratios of reovirus preparations were done as described previously (24). To determine infectious

titers in other experiments, a modified procedure was used. Prior to addition of virus, the monolayers were washed to remove serum with PBS plus 2 mM $MgCl_2$. After a 1-h attachment period, the monolayers were covered with 2 ml of 1% Bacto Agar and serum-free medium 199 containing 10 μg of trypsin per ml (Sigma). Plaques were counted 2 days later.

Infectivity experiments. Single-step growth curves were determined as described elsewhere (15). Endpoint experiments with NH_4Cl were performed as for single-step growth curves except that only 0- and 24-h time point samples were harvested and 20 mM NH_4Cl was included in the culture medium. Endpoint experiments with E-64 (Sigma) and pepstatin A (Sigma) were performed as follows. L cells at 4×10^5 cells/ml were dispensed in 2-dram vials and pretreated for 2 h at 37°C with 300 μM E-64 or 30 μM pepstatin A (each dissolved in dimethyl sulfoxide), or with dimethyl sulfoxide alone (for samples without inhibitor). After pretreatment, cells were chilled at 4°C for ≥15 min, the growth medium was removed, and virus particles were added at 3 PFU/cell. Adsorption proceeded for 1 h at 4°C, after which the inoculum was removed, and the original medium (with or without inhibitor) was added back to each vial. Vials were then transferred to a 37°C incubator, and 0- and 24-h time point samples were harvested by freezing.

Hemolysis and transcription. The capacity of reovirus particles to lyse erythrocytes was measured by a spectrophotometric assay for hemoglobin release (15, 39). The capacity of reovirus particles to mediate transcription of the viral mRNAs in vitro was measured by a radiometric assay for incorporation of [α-^{32}P]GTP into acid-precipitable material (36).

Heat inactivation. Viral particles at a concentration of 4×10^7 particles/ml in 500 μl of virion buffer were incubated at 52°C for 1 h or were kept on ice as a control. Heat treatment was ended by transferring the 52°C samples onto ice, and infectious titers were determined for all samples by plaque assay. The decrease in infectivity due to heat inactivation was expressed as the difference between the $\log_{10}$ titers of each heat-treated sample and the corresponding control sample.

Construction of T1L and T3D σ3 chimeras. DNA clones of the T1L and T3D S4 genes, inserted into pBluescript KS$^+$ (Stratagene, La Jolla, Calif.) at the *Eco*RI site, were cleaved with *Bsa*I and *Sty*I (both within the S4 gene) or with *Sty*I and *Eco*RV (the latter within the vector beyond the 3′ end of the S4 plus strand) to obtain middle (S4 nucleotides 552 to 791, corresponding to σ3 amino acids 186 to 265) or C-terminal (S4 nucleotides 792 to 1095, corresponding to σ3 amino acids 266 to 365) fragments of S4, respectively. These fragments were exchanged between the T1L and T3D S4 constructs to generate chimeras as shown in Fig. 10A. The chimeric S4 genes were subcloned into the pEV/35K/polybsmcr plasmid (34), and the resulting constructs were used to express each σ3 protein in insect cells by using a novel baculovirus system (28). Protein was labeled at 40 h postinfection with 25 μCi of [^{35}S]methionine/cysteine per ml, and 8 h later cells were harvested as described above.

RESULTS

Expression of recombinant σ3 protein in insect cells. To obtain high levels of σ3 expression for stoichiometric recoating of ISVPs, we constructed a recombinant baculovirus containing a cDNA copy of the S4 gene from reovirus T3D under control of the baculovirus polyhedrin promoter. At 48 h after infection with the recombinant baculovirus, insect cells were harvested and lysed. This treatment, followed by centrifugation at 500 × *g*, rendered a soluble supernatant (cytoplasmic fraction) and a pellet containing nuclei and insoluble material. SDS-PAGE and immunoblot analyses of these two fractions (Fig. 1 and data not shown) confirmed high levels of σ3 expression and revealed that most σ3 was in the pellet. This distribution could indicate either that σ3 was insoluble or that it had been localized to the nucleus in insect cells as previously observed for σ3 expressed in HeLa cells from an S4 cDNA (56) and in L cells after reovirus T3D infection (43). To distinguish between these possibilities, we resuspended the pellet and disrupted the nuclei with a series of buffers containing increasing amounts of salt. After centrifugation at 22,000 × *g*, SDS-PAGE of each new supernatant (nuclear lysate) and pellet fraction demonstrated recovery of σ3 in the supernatant, with more σ3 protein recovered at higher salt concentrations (data not shown). These findings suggest that σ3 was recovered in the initial pellet because of its localization to the nucleus in insect cells. In subsequent experiments, buffer containing 0.5 M NaCl was used to release σ3 from the pellet (as shown in Fig. 1) since higher concentrations did not improve recovery and were a concern for binding experiments.

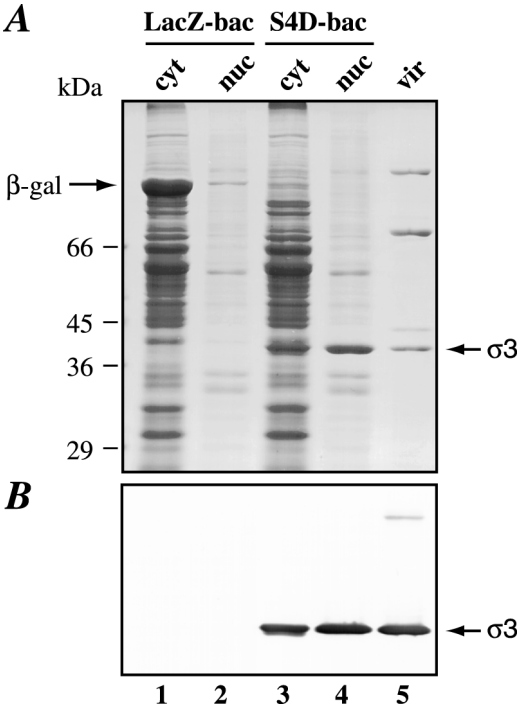

FIG. 1. Expression of σ3 in insect cells by using recombinant S4D-baculovirus. (A) Cytoplasmic (cyt) and nuclear lysate (nuc) fractions from Sf21 cells infected with LacZ-baculovirus (lanes 1 and 2) or S4D-baculovirus (lanes 3 and 4) were subjected to SDS-PAGE and Coomassie blue staining. A sample of reovirus T3D virions (vir; lane 5) was included to give a size marker for σ3. The positions of β-galactosidase (β-gal) and σ3 proteins are indicated by arrows. Molecular weight markers (sizes in kilodaltons) are indicated at the left. (B) The lysate fractions analyzed in panel A were subjected to SDS-PAGE followed by immunoblot analysis using σ3-specific monoclonal antibody 4F2 (53). The origin and significance of the high-molecular-weight band in lane 5 of panel B remain unconfirmed; however, this band is likely to represent a dimeric form of σ3 that resists disruption in preparation for electrophoresis. This form of σ3 may arise during particle preparation and/or storage since it is seen only with purified particles (also see Fig. 2B, lanes 1 and 3).

Stoichiometric recoating of ISVPs with recombinant σ3. To determine if baculovirus-expressed T3D σ3 protein can bind to ISVPs, purified ISVPs of reovirus T1L (generated from virions by in vitro CHT digestion and chosen over T3D ISVPs for their greater stability) were incubated with nuclear lysate from σ3-expressing insect cells. After incubation, the particles were subjected to centrifugation in a preformed CsCl gradient to separate soluble σ3 from any that was particle associated. SDS-PAGE and immunoblot analyses revealed that σ3 had bound to the particles and remained bound through centrifugation (Fig. 2). Different ratios of σ3-containing lysate and ISVPs led to different extents of σ3 binding (data not shown). With excess lysate, however, the amount of bound σ3 appeared to approximate that present in virions (Fig. 2), suggesting that nearly all potential binding sites for σ3 had been occupied. To quantify the extent of recoating, SDS-PAGE followed by Coomassie blue staining and densitometry was performed with both native virions and ISVPs that appeared to have been fully recoated with σ3. For each sample, the intensity of the σ3 band was expressed relative to that of the λ-protein band. Comparison of σ3/λ ratios indicated that the σ3 content of the recoated particles was equivalent to that of virions (Table 1), consistent with stoichiometric recoating.

Measurements of buoyant density were made to obtain additional evidence that complete recoating of ISVPs had been

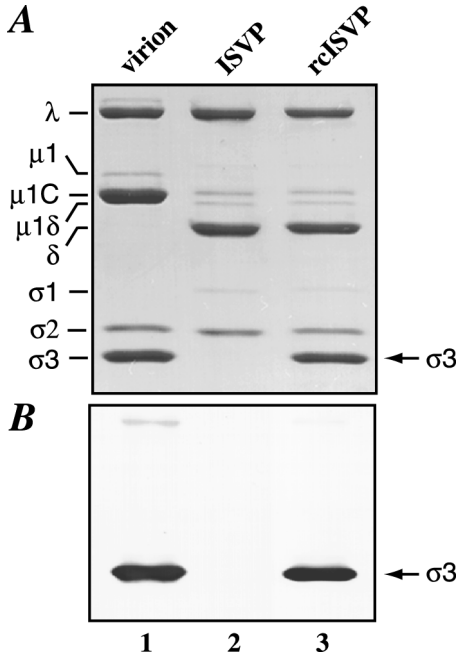

FIG. 2. SDS-PAGE and immunoblot analysis of rcISVPs. T1L ISVPs (2.5×10^{12}) were incubated with the nuclear fraction from 5×10^6 Sf21 cells infected with S4D-baculovirus. rcISVPs were purified by centrifugation through a CsCl density gradient and dialyzed extensively against virion buffer. Virions (lane 1), ISVPs (lane 2), and rcISVPs (lane 3) (5×10^{10} each) were subjected to SDS-PAGE and Coomassie blue staining (A) or immunoblotting with the σ3 monoclonal antibody 4F2 (53) (B).

approximated with baculovirus-expressed σ3. Virions and ISVPs contain the same complement of nucleic acids, but virions have a higher protein content due to the presence of σ3 and thus exhibit a buoyant density in CsCl (1.36 g/cm^3) lower than that of ISVPs (1.38 g/cm^3) (24, 30). Recoated particles migrated at a buoyant density of 1.361 g/cm^3 ($\pm$0.003, $n = 3$), equivalent to that of native virions, suggesting that stoichiometric or near-stoichiometric recoating had been achieved.

Henceforth, we use the term rcISVPs to refer to ISVPs that have been recoated with approximately stoichiometric levels of baculovirus-expressed σ3 protein. It is important to note that rcISVPs are similar to virions in that they contain a full complement of σ3 but similar to ISVPs in that they contain μ1/μ1C mostly cleaved at the δ-ϕ junction. The implications of these features for the structure and function of rcISVPs are addressed below.

TABLE 1. Amounts of σ3 protein in rcISVPs

Trial[a]	Particle type	Prepn[b]	σ3/λ[c] (mean ± SD)
1	Virion, T1L		1.51 ± 0.08
	rcISVP	A	1.51 ± 0.02
2	Virion, T1L		1.26 ± 0.04
	rcISVP	B	1.28 ± 0.12
3	Virion, T1L		1.27 ± 0.03
	rcISVP	C	1.30 ± 0.03

[a] Each trial represents an individual SDS-polyacrylamide gel.
[b] Three independent preparations of rcISVPs (A, B, and C) were analyzed in the three trials.
[c] Proteins from purified virus particles were separated by SDS-PAGE and visualized by Coomassie blue staining. The σ3 and λ protein bands were quantitated by laser densitometry (Molecular Dynamics), and the σ3/λ ratio was calculated for each particle sample. The values shown were determined from three lanes of each particle type that were analyzed per gel.

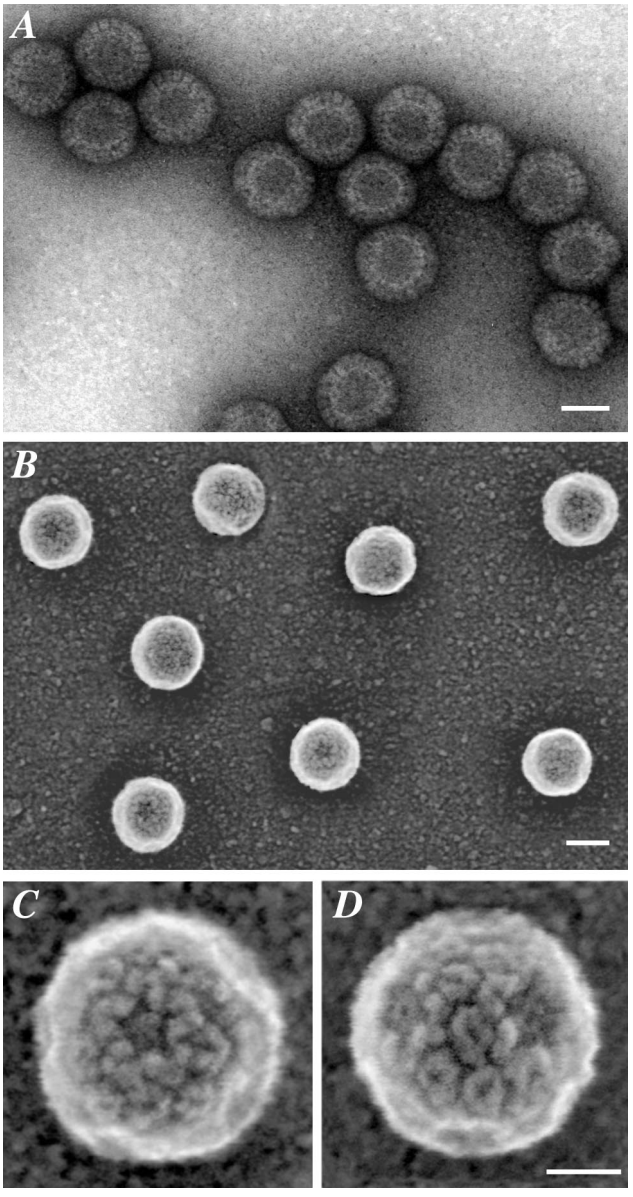

FIG. 3. Conventional TEM and cryo-SEM of rcISVPs. (A) Population of negatively stained rcISVPs viewed by conventional TEM at a magnification of ×100,000. Bar, 50 nm. (B) Population of chromium-coated rcISVPs viewed by high-resolution cryo-SEM at a magnification of ×100,000. Bar, 50 nm. (C and D) Single chromium-coated rcISVPs viewed by cryo-SEM at a magnification of ×300,000. Particles oriented near a fivefold axis (C) and near a twofold axis (D) are shown. Bar, 25 nm.

The σ3 coats of virions and rcISVPs appear structurally identical, as determined by electron microscopy and 3-D image reconstruction. rcISVPs were analyzed by conventional TEM after negative staining to compare them to native virions and ISVPs. A homogeneous population of particles very similar in morphology to virions was observed (Fig. 3A). Measured diameters of the particles ranged from 72 to 76 nm (data not shown), which is consistent with the diameter of native virions previously determined by negative-stain TEM (7, 24). Like virions (24), rcISVPs displayed a smooth perimeter with char-

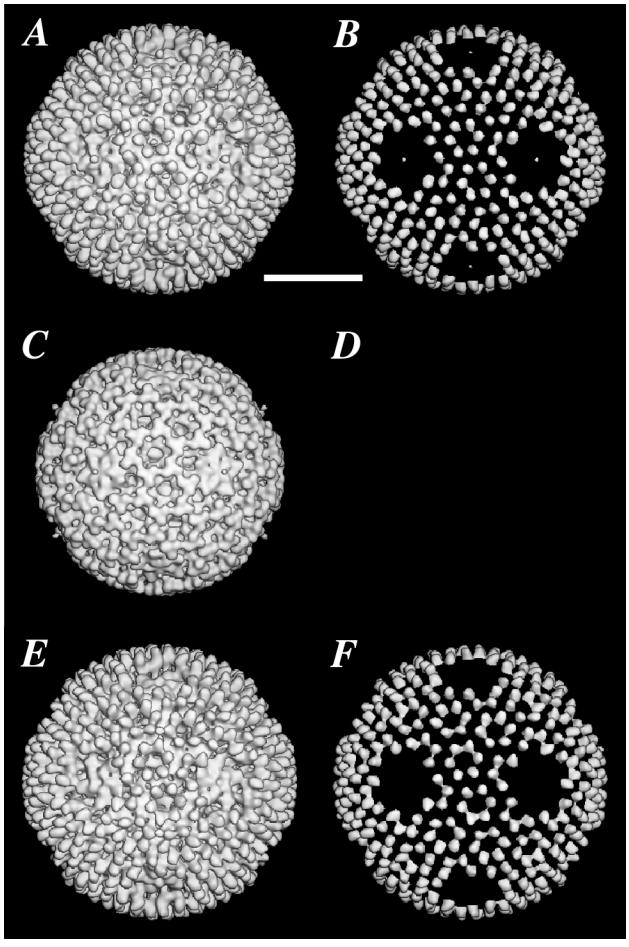

FIG. 4. 3-D image reconstruction of rcISVPs obtained from cryo-TEM images (E and F; 33-Å resolution) compared with previously reported reconstructions of T1L virions (A and B; 28-Å resolution) and ISVPs (C and D; 29-Å resolution) (21). (A, C, and E) Surface-shaded views down a twofold axis of symmetry for each particle. (B, D, and F) Same views as in panels A, C, and E except that the reconstructions were radially cropped to remove all densities below 41 nm, thereby isolating features attributable to σ3 in the display. Bar, 30 nm.

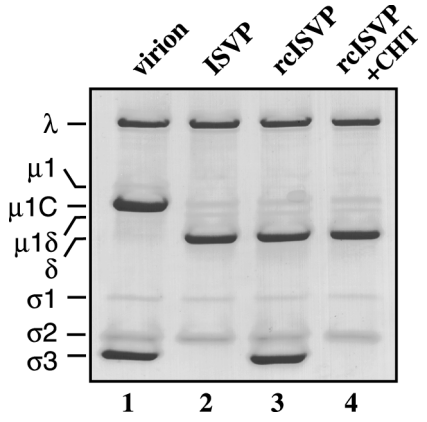

FIG. 5. Regeneration of ISVPs from rcISVPs. rcISVPs (7.5×10^{10}) were treated with CHT at 200 μg/ml for 20 min at 37°C in a final volume of 20 μl. The reaction was stopped by adding 1 mM phenylmethylsulfonyl fluoride and transferring the sample to 4°C. After disruption in sample buffer, the CHT-treated sample was analyzed by SDS-PAGE and Coomassie blue staining (lane 4), as was a sample containing the same number of untreated rcISVPs (lane 3). Equivalent numbers of purified virions (lane 1) and the purified ISVPs from which the rcISVPs were generated (lane 2) were also run on the gel for comparison.

acteristic flattened edges that arise at fivefold axes where the μl-σ3 lattice is interrupted by λ2 (21, 37).

We used cryo-SEM to compare the organization of σ3 subunits on individual rcISVPs and virions. This technique shows individual proteins on the surfaces of reovirus particles at a resolution of 2 to 4 nm (13). rcISVPs exhibited characteristic rings of protein distributed over much of their surface and incomplete rings surrounding the fivefold axes (Fig. 3B to D). These features correspond to complete and partial hexamers of σ3 (see below), consistent with the results of the previous cryo-SEM study of reovirus virions (13). As no clear differences distinguish the cryo-SEM images of rcISVPs and native virions (13), these findings suggest that a native σ3 coat was reconstituted in rcISVPs.

The σ3 coat in rcISVPs was visualized at higher resolution in three dimensions by using cryo-TEM techniques and image reconstruction procedures for icosahedral particles. At 33-Å resolution, the 3-D reconstruction revealed that rcISVPs have a capsid structure very similar to that of native virions (Fig. 4). The 600 finger-like structures that project >40 Å above the top of the μ1 protein layer are believed to represent 600 molecules of σ3 (21). These projections are arranged identically in virions (Fig. 4A and B) and rcISVPs (Fig. 4E and F), that is, according to T=13(laevo) icosahedral symmetry with complete hexamers (six σ3 subunits) surrounding the P3 channels and partial hexamers (four σ3 subunits) forming an incomplete ring around each P2 channel (21, 37). In rcISVPs as in virions, one σ3 subunit in each partial hexamer appears to form contacts with the λ2 subunit(s) that projects into the P2 channel (21, 37). The features attributable to σ3 in the reconstruction of rcISVPs thus confirm those observed with individual particles by conventional TEM and cryo-SEM and support the conclusion that the σ3 subunits in these particles mediate interactions with other outer-capsid proteins that are very similar to those in native virions.

Regeneration of ISVPs from rcISVPs. In vitro treatment of virions with alkaline proteinases such as CHT or trypsin can remove σ3 from the particle surface and cleave μ1/μ1C at the δ-ϕ junction, thus generating ISVPs (7, 30, 45). Several observations suggest that this process is analogous to the early proteolytic steps during reovirus infection (16, 48). To determine if rcISVPs can be similarly processed by alkaline proteinases, we digested purified rcISVPs under conditions of CHT treatment designed to generate ISVPs (200 μg of CHT per ml for 20 min at 37°C). SDS-PAGE of the reaction sample revealed that σ3 was completely removed from rcISVPs (Fig. 5) but the remaining structural proteins were cleaved little if at all. Treatments with trypsin gave identical results (data not shown). The buoyant density of CHT-treated particles was measured at 1.375 g/cm^3 ($\pm$0.001, n = 3), consistent with the value of 1.38 g/cm^3 characteristic of ISVPs. Hence, our results show that ISVPs can be regenerated from rcISVPs by in vitro treatment with alkaline proteinases and that addition and removal of σ3 has little if any adverse effect on the other capsid proteins.

rcISVPs are fully infectious. Structural similarities between rcISVPs and virions suggest that rcISVPs will provide a useful tool for analyzing σ3 structure in virions. However, meaningful studies of the function and fate of virion-bound σ3 in vivo depend on the extent to which rcISVPs remain infectious. The relative infectivity of rcISVPs was determined in plaque assays in which L cells were infected with purified virions, rcISVPs, or the ISVPs that had been used to generate the rcISVP prepa-

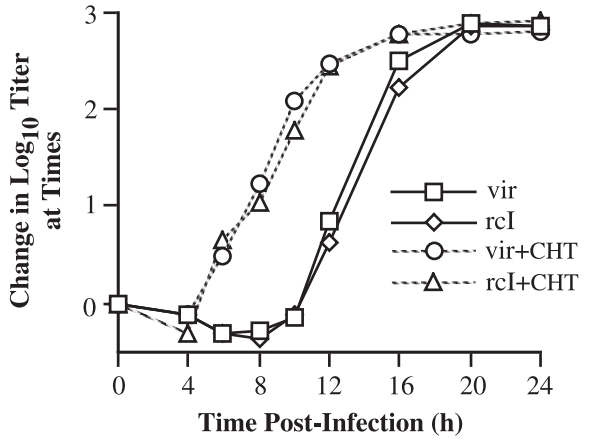

FIG. 6. Single-step growth curve after infection with rcISVPs. T1L virions (vir), rcISVPs (rcI), or ISVPs generated by CHT digestion of each (vir+CHT or rcI+CHT, respectively) were used to infect L cells at 3 PFU/cell. After 1 h at 4°C, unbound virus was removed, and infected cells were added to 2-dram vials containing growth medium. Infected cells were incubated at 37°C and then harvested at different times postadsorption for determination of infectious titers by plaque assay. The change in $\log_{10}$ titer over time is expressed relative to the corresponding 0-h sample. Each point represents the average of two independent infections.

rations. Similar determinations were made with CHT digests of purified rcISVPs designed to regenerate ISVPs. Infectivity was correlated with particle concentration to obtain the relative infectivity of each preparation expressed as a particle/PFU ratio. We found the mean relative infectivities of virions and rcISVPs to be very similar: 74 particles/PFU for T1L virions and 70 particles/PFU for three preparations of rcISVPs. The mean relative infectivities of the corresponding ISVPs were also very similar: 69 particles/PFU for T1L ISVPs and 82 particles/PFU for CHT digests of two preparations of rcISVPs. These results indicate that neither addition of σ3 to generate rcISVPs nor its subsequent removal to regenerate ISVPs has a substantial effect on infectivity.

Virions and rcISVPs exhibit identical replication kinetics. There is a characteristic difference in the kinetics of viral growth when cells are infected with reovirus virions or ISVPs. The lag phase extends for 8 to 10 h postadsorption with virions but for only 4 to 6 h with ISVPs (3, 15, 18, 50). The absence of σ3 and cleavage of μ1/μ1C at the δ-ϕ junction represent two major structural differences between ISVPs and virions that could be related to the different kinetics. Since rcISVPs contain σ3 as do virions, but cleaved μ1/μ1C as do ISVPs, we used them to determine whether either of these structural features affects the lag phase in single-cycle growth curves. Virions, rcISVPs, and ISVPs generated from each by in vitro CHT treatment were adsorbed to L cells at 4°C, and samples were harvested periodically over a 24-h period at 37°C for measurement of infectious titers. Infections with virions and rcISVPs demonstrated nearly identical growth kinetics, with the lag phase ending near 10 h postadsorption (Fig. 6). Infections with ISVPs derived from virions or rcISVPs also exhibited indistinguishable kinetics, but the lag phase ended at about 4 h postadsorption (Fig. 6). Hence, the presence or absence of σ3, and not the δ-ϕ cleavage of μ1/μ1C, appears to be the primary determinant of growth kinetics for infections with the different particle types.

Infections with rcISVPs are blocked by NH_4Cl and E-64 but not pepstatin A. Cells treated with inhibitors of acid-dependent lysosomal proteinases, such as the weak base NH_4Cl and cysteine proteinase inhibitor E-64, resist infections with reovirus virions at least in part because cleavages of σ3 and/or μ1/μ1C are blocked (3, 15, 50). These agents, however, have no effect on infections with ISVPs (3, 15, 50). The requirement for proteolysis with virions, but not ISVPs, is thought to partially explain the different kinetics of growth after infections with these particles. Since most μ1/μ1C molecules are already cleaved at the δ-ϕ junction in rcISVPs, it was important to determine whether infections with these particles are also dependent on cleavages by the acid-dependent cysteine proteinases. Virions, rcISVPs, and ISVPs generated from each by in vitro CHT treatment were adsorbed to L cells at 4°C. Infections then proceeded at 37°C in the presence or absence of 20 mM NH_4Cl or 300 μM E-64, and infectious titers were determined after 24 h. As expected, infections with virions were blocked by NH_4Cl or E-64 whereas infections with virion-derived ISVPs were not blocked by either compound (Fig. 7A and B). Similarly, infections with rcISVPs were blocked, but infections with rcISVP-derived ISVPs were not blocked, by either compound (Fig. 7A and B). Thus, virions and rcISVPs, despite prior cleavage of μ1/μ1C at the δ-ϕ junction in the latter, are similarly dependent on the processing of σ3 by acid-dependent cysteine proteinases for productive infection.

Unlike inhibitors of acid-dependent cysteine proteinases, pepstatin A, a specific inhibitor of aspartic proteinases like cathepsin D, has no effect on reovirus replication (32). This result indicates that degradation of σ3 is a process involving a specific subset of cellular proteinases. To determine if aspartic proteinase activity is also dispensable for infections with rcISVPs, L cells were adsorbed at 4°C with virions, rcISVPs, or CHT-generated ISVPs from each. Infections then proceeded at 37°C in the presence or absence of 30 μM pepstatin A, and infectious titers were measured at 24 h. This inhibitor did not affect the growth of any of the particle types (Fig. 7C). Coupled with the NH_4Cl and E-64 results (Fig. 7A and B), this finding suggests that σ3 in rcISVPs is susceptible to cleavage by the same subset of cellular proteinases as it is in virions.

rcISVPs cannot undergo in vitro activation to mediate hemolysis or transcription of the viral mRNAs. In vitro, ISVPs but not virions can be activated to interact with lipid bilayers (9, 15, 27, 35, 39, 52) and to transcribe the viral mRNAs (8, 10, 15, 19, 22, 30, 45). Productive infection in vivo depends on analogous activities. Available data (see above) suggest that virions require proteolysis for infection in order to generate subvirion particles that can undergo activation to mediate these activities. dpSVPs, which lack σ3 but have most molecules of μ1/μ1C uncleaved at the δ-ϕ junction as in virions, can also be activated to interact with lipid bilayers and to mediate transcription in vitro in the absence of further proteolysis (15). Thus, the δ-ϕ cleavage appears to be dispensable for these activities. Because rcISVPs, in contrast to other particles, have a full σ3 coat and most μ1/μ1C molecules cleaved at the δ-ϕ junction, we used them to determine whether the presence of σ3 influences the activation of particles to mediate hemolysis and transcription.

As in preceding cell culture experiments, assays were performed with virions, rcISVPs, and CHT-generated ISVPs from each. CsCl was included in samples to accelerate the structural changes in outer-capsid proteins that accompany membrane permeabilization and transcriptase activation (8, 11, 14, 52). Lysis of erythrocytes (hemolysis) is believed to represent a simple model by which the interactions with lipid bilayers required for reovirus entry into cells can be investigated (15, 39). Hemolysis assays performed in this study indicate that ISVPs but not virions or rcISVPs can be activated to interact with lipid bilayers (Fig. 8). Activation of the viral transcriptase is

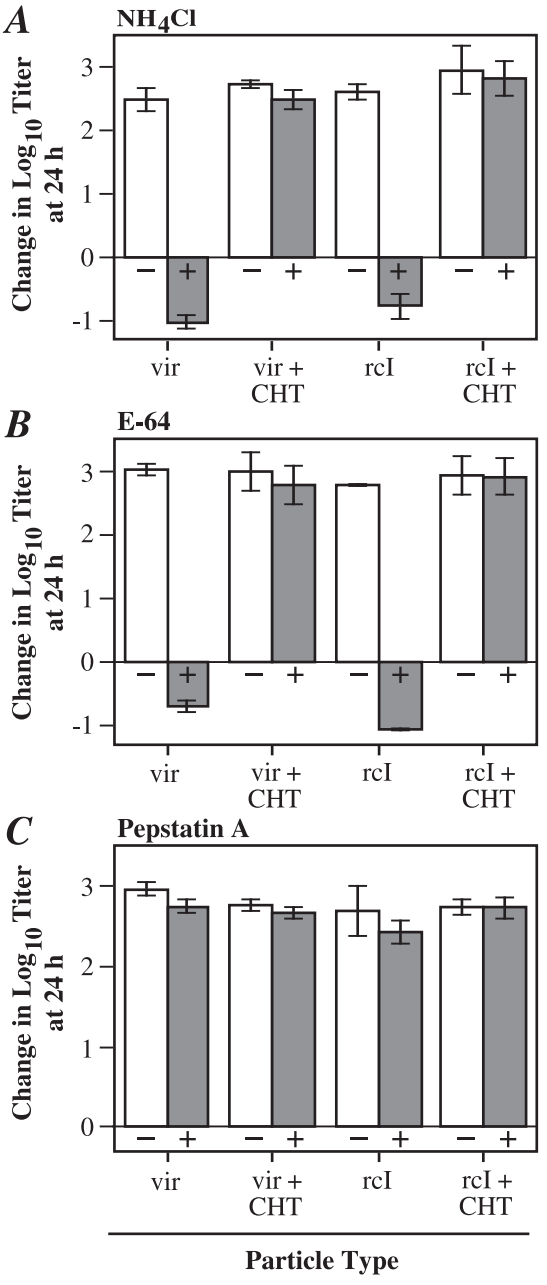

FIG. 7. Viral growth in the presence of NH_4Cl, E-64, or pepstatin A after infection with rcISVPs. T1L virions, rcISVP, or their corresponding ISVPs (vir + CHT or rcI + CHT, respectively) were used to infect L cells at 3 PFU/cell. After attachment for 1 h at 4°C, infected cells were incubated at 37°C for 0 or 24 h in the absence (−; open bars) or presence (+; shaded bars) of 20 mM NH_4Cl (A), 300 μM E-64 (B), or 30 μM pepstatin A (C). Infectious titers were determined by plaque assay. The change in $\log_{10}$ titer after 24 h is expressed relative to the corresponding 0-h sample. Each bar represents the average ± standard deviation of three independent infections.

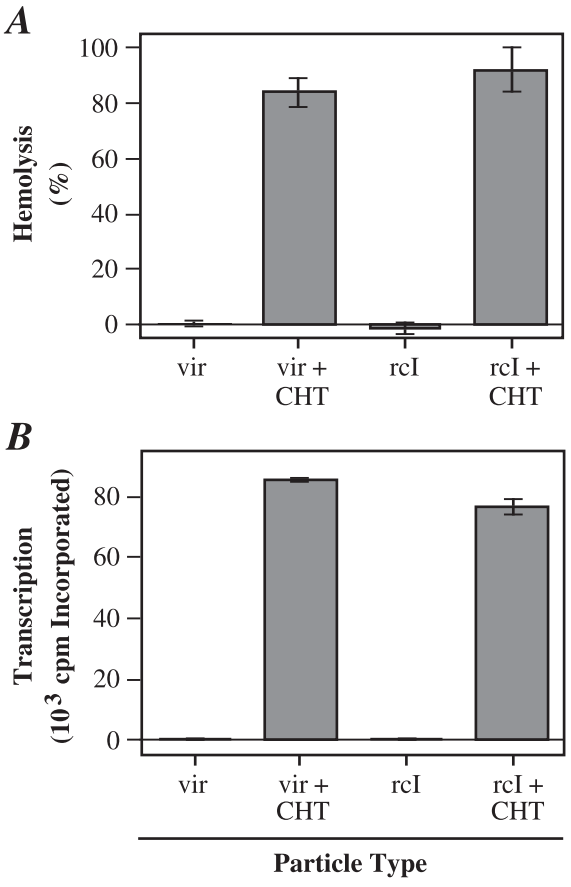

FIG. 8. Capacity of rcISVPs to be activated to mediate hemolysis or transcription. Each bar represents the mean ± standard deviation from three trials. (A) A 3% solution of calf erythrocytes was incubated with 5×10^{10} T1L virions (vir), rcISVPs (rcI), or ISVPs generated by CHT digestion of each (vir + CHT or rcI + CHT, respectively) at 37°C for 30 min in the presence of 200 mM CsCl as an accelerant (8, 15). The extent of hemolysis was expressed as a percentage of that obtained by hypotonic lysis. (B) T1L virions, rcISVPs, or their respective ISVPs (5×10^{10} each) were incubated with a transcription mixture including 2 mM ribonucleoside triphosphate, 1.13 μCi of [α-^{32}P]GTP, and 200 mM CsCl. The incorporation of ^{32}P into viral transcripts was measured after precipitation with trichloroacetic acid (36).

thought to require changes in particle structure that follow and/or accompany membrane permeabilization (10, 14, 19, 21, 22, 27, 30, 39). Transcriptase assays performed in this study indicate that ISVPs but not virions or rcISVPs can be activated to produce viral transcripts (Fig. 8). Taken together, the hemolysis and transcription results suggest that the presence or absence of σ3 protein, and not the δ-φ cleavage of μ1/μ1C, is the primary determinant of whether a given particle type can be activated to interact with lipid bilayers and to transcribe the viral mRNAs.

rcISVPs and virions are similarly thermostable. Reovirus virions are more resistant to heat inactivation than ISVPs (44). This property may enable virions to survive a wider range of conditions outside host organisms, thereby improving transmission of the virus between hosts (41). rcISVPs were analyzed to distinguish the roles of σ3 and cleavage of μ1/μ1C at the δ-φ junction in determining the thermostability of particles. Virions, rcISVPs and ISVPs derived from each by in vitro CHT treatment were incubated at either 52 or 4°C in virion buffer for 1 h, and samples were then assayed for infectivity (Fig. 9). After 1 h at 52°C, ISVP samples exhibited a large decrease in titer, to <0.01% of that of the 4°C controls. In contrast, the titers of virions and rcISVPs decreased only to ~10% of control levels. Thus, virions and rcISVPs exhibited comparable greater thermostability than their respective ISVPs. The CHT present in the ISVP samples was not responsible for the loss of infectivity observed with heating since inactivation experiments performed with purified T1L ISVPs, with or without added CHT, gave very similar results (reference 44 and data not

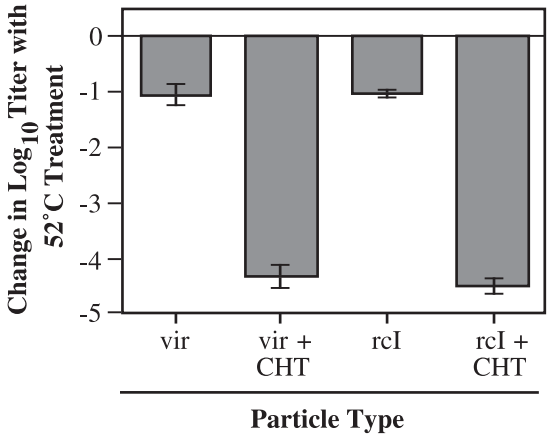

FIG. 9. Sensitivity of rcISVPs to heat inactivation. T1L virions (vir), rcISVPs (rcI), or ISVPs generated by CHT digestion of each (vir + CHT or rcI + CHT, respectively) were subjected to heat inactivation at 52°C for 1 h. Corresponding samples were kept at 4°C as controls. Infectious titers were determined by plaque assay, and the change in $\log_{10}$ titer with heat treatment is expressed relative to the corresponding 4°C sample. Each bar represents the mean ± standard deviation from three trials.

shown). These results demonstrate that σ3 is the primary determinant of the different thermostabilities of virions and ISVPs and that cleavage of μ1/μ1C at the δ-ϕ junction has little or no effect on this property. These conclusions are consistent with a previous analysis showing that the S4 gene (which encodes σ3) determines strain-specific differences in the thermostability of reovirus virions (20).

Analysis of σ3 cleavage rate by recoating genetics using chimeric σ3 proteins bound to ISVPs. Proteolysis of reovirus outer-capsid proteins by luminal alkaline proteinases in the mammalian small intestine is required for at least some reovirus strains to adhere to M cells and infect intestinal target tissues (1, 6). During the course of experiments to dissect the cascade of cleavages that occur during alkaline proteolysis of σ3, we treated purified T1L and T3D virions in vitro with endoproteinase Lys-C (EKC), a serine alkaline proteinase, and observed a difference in the rate at which full-length σ3 protein was cleaved in these two strains, the σ3 protein in T1L virions being cleaved faster than that in T3D virions (29). A genetic analysis using T1L × T3D reassortants indicated that the determinants of this difference reside within the two σ3 proteins themselves (29). To localize these determinants within σ3, we took advantage of our method for recoating ISVPs with baculovirus-expressed σ3 protein. Eight distinct types of [^{35}S]methionine/cysteine-labeled σ3 protein were separately expressed and used for recoating T1L ISVPs: T1L σ3, T3D σ3, and six chimeric proteins generated by exchanging amino acids 1 to 185, 186 to 265, and/or 266 to 365 between the T1L and T3D σ3 proteins (Fig. 10A). The resulting particles were purified from CsCl gradients and subjected to EKC cleavage, followed by visualization and quantitation of full-length σ3 protein by SDS-PAGE and phosphorimaging (Fig. 10B). The extent of σ3 cleavage was assessed by comparing the intensities of the full-length σ3 bands from EKC-treated and untreated samples of each particle preparation (Fig. 10C). The results demonstrate that the C-terminal 100 amino acids of σ3 contain the primary determinants of the different rates of EKC cleavage of T1L and T3D σ3: all σ3 proteins with the C-terminal region from T1L exhibited a higher rate of cleavage than those with the C-terminal region from T3D (Fig. 10C). Interestingly, the N-terminal and middle regions of σ3 made secondary contributions to cleavage rate, but in the directions opposite those expected from behaviors of the parental proteins: chimeric σ3 proteins containing the N-terminal and/or middle regions from T3D exhibited an increased rate of cleavage, whereas chimeric σ3 proteins containing one or both of those regions from T1L exhibited a decreased rate of cleavage. These findings suggest that different regions of σ3 can contribute to the overall rate of cleavage but indicate a more prominent role for C-terminal sequences. The latter conclusion concurs with that from another recent study, which showed that a mutation near the C

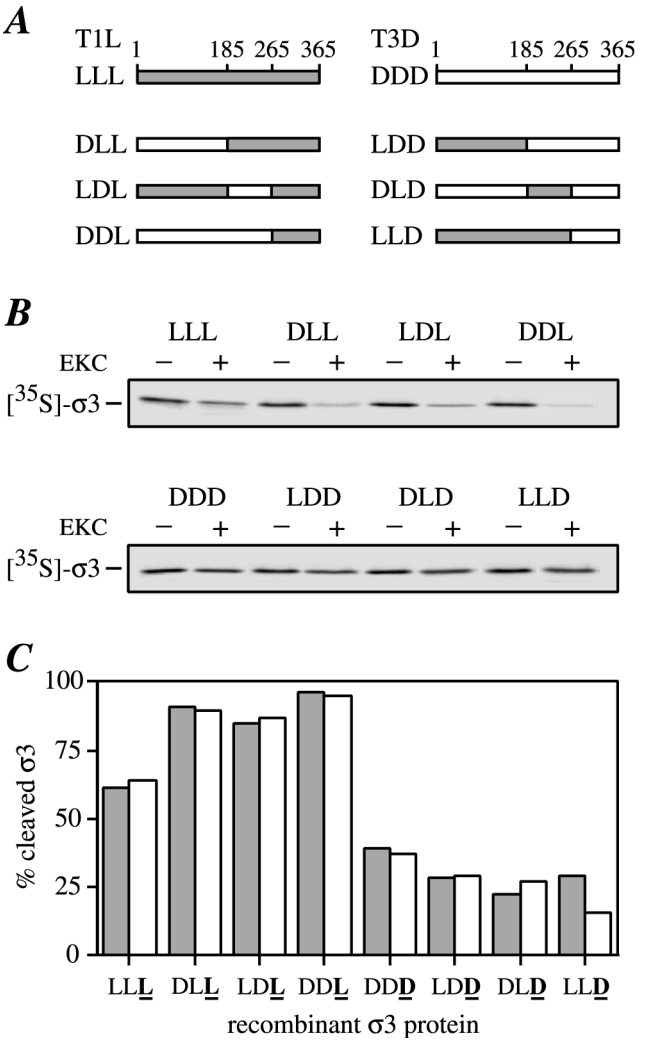

FIG. 10. Analysis of σ3 cleavage rate by recoating genetics using chimeric σ3 proteins bound to ISVPs. (A) T1L and T3D σ3 proteins, as well as six σ3 chimeras generated by exchanging N-terminal, middle, and C-terminal regions (junctions indicated by amino acid number) of the σ3 proteins of reoviruses T1L and T3D, were expressed in insect cells (see Materials and Methods). Each type of σ3 protein is designated by three letters indicating the origin (L or D) of the three regions. (B) [^{35}S]methionine/cysteine-labeled σ3 proteins of the eight types shown in panel A were separately bound to T1L ISVPs, which were then purified in a CsCl gradient and dialyzed into virion buffer. The purified particles were subsequently treated with EKC (20 μg/ml) for 1 h at 37°C, and the reaction was stopped using 1 mM TLCK (Sigma). Equivalent numbers of EKC-treated (+) and untreated (−) particles were analyzed by SDS-PAGE and phosphorimaging. The bands corresponding to full-length σ3 are shown from two representative gels on which all eight types of σ3-containing particles were analyzed. (C) The σ3 bands were quantitated by phosphorimaging, and the amount of full-length σ3 remaining in each EKC-treated sample was expressed as a percentage of that in the corresponding untreated sample. The filled and open bars indicate measurements from two pairs of samples for each particle preparation.

TABLE 2. Summary of rcISVP properties[a]

Particle type	Presence of σ3	Cleavage at δ-ϕ	Long lag phase	Sensitivity to NH_4Cl and E-64	Block to activation of hemolysis and transcription	Thermostability
Virion	+	−	+	+	+	+
rcISVP	+	+	+	+	+	+
dpSVP[b]	−	−	−	−	−	−
ISVP	−	+	−	−	−	−

[a] See text for more complete descriptions of the particle types, properties, and behaviors.
[b] Findings are from reference 15 except for the thermostability data, which were generated for this report (data not shown).

terminus of σ3 affects the proteinase sensitivity of the virion-bound protein in a reovirus mutant selected during persistent infection (55).

DISCUSSION

Assembly of σ3 into virions in vivo and in vitro. In reovirus-infected cells, mature virions undergo a regulated process of assembly that remains poorly characterized. One observation, however, is that outer-capsid assembly is blocked and core-like particles accumulate when cells are infected at nonpermissive temperatures with virus containing a temperature-sensitive lesion in the S4 gene (*ts*G453) (38, 47). This finding suggests that the μ1 protein cannot be assembled into particles in the absence of functional σ3. In fact, μ1 and σ3 are known to form complexes in solution (33), and this interaction modifies the conformation of σ3 such that its proteinase sensitivity is increased to the level seen in virions (46). In addition, the μ1 protein in μ1-σ3 complexes becomes susceptible to cleavage near its N terminus, yielding fragments μ1N and μ1C through what is thought to be an autocatalytic mechanism (42, 51). Together, these findings suggest that during assembly of virions in infected cells, μ1-σ3 complexes are formed first, which modifies the conformation of both μ1 and σ3 and allows these complexes to bind to nascent particles (38, 47).

The procedure for generating rcISVPs described in this study involves a mechanism for σ3 assembly into particles distinct from that observed in vivo. In our in vitro system, an apparently native σ3 coat is reconstituted in rcISVPs after soluble σ3 binds to the preformed μ1 lattice in ISVPs. Hence, σ3 does not strictly require the prior formation of μ1-σ3 complexes for assembly into particles. Given this fact, we infer that the necessity for forming μ1-σ3 complexes before assembly onto core-like particles in infected cells most likely reflects the need for σ3 binding to induce μ1 into a specific conformation that is competent to self-associate or to interact with other viral components in forming the outer capsid. The mechanism for assembling σ3 onto ISVPs, which we have exploited, is also demonstrated by ISVP-like particles from cellular lysosomes when they undergo recoating with soluble σ3 from the cytoplasm or nucleus upon disruption of reovirus-infected cells (2, 16, 50).

Binding to σ3 is not blocked by cleavages of μ1 at the μ1N-μ1C and δ-ϕ junctions in ISVPs. As noted above, the μ1 molecules in virions have undergone several changes in structure relative to soluble μ1, including conformational changes and a cleavage near their N termini to generate the μ1N and μ1C fragments by which most μ1 molecules are represented in virions. Moreover, when ISVPs are subsequently generated from virions by proteolysis, the μ1/μ1C molecules undergo an additional cleavage near their C termini to generate fragments μ1δ/δ and ϕ (40). It was conceivable that one or more of these changes might have modified μ1 such that, in its ISVP-bound form, it was no longer competent to bind soluble σ3 protein. However, because soluble σ3 can bind to μ1δ/δ and/or ϕ in ISVPs, as directly shown in this study and previously (2, 46), the sites in μ1 that mediate σ3 binding cannot have been irreversibly modified as a consequence of any of the changes in μ1 that accompany complex formation, μ1N-μ1C cleavage, particle binding, or δ-ϕ cleavage. In partial support of this conclusion, a 3-D reconstruction of dpSVPs, in which very few μ1/μ1C molecules have been cleaved at the δ-ϕ junction (15), failed to demonstrate any clear structural differences from ISVPs (54), suggesting that the δ-ϕ cleavage in ISVPs has little effect on μ1 conformation.

Effect of σ3 on functional properties of reovirus particles in vitro and in vivo. After addition of σ3 to ISVPs, to generate rcISVPs, these particles behave like virions in all of the functional properties tested in this study (summarized in Table 2). Thus, σ3 is a key determinant of particle behavior for each of these properties. An important structural distinction between virions and rcISVPs is that the latter contain most molecules of μ1/μ1C cleaved at the δ-ϕ junction, like ISVPs. As a result, our findings with rcISVPs also indicate that cleavage of μ1/μ1C at the δ-ϕ junction is not an important determinant of the differences in behavior between virions and ISVPs studied here. Previous experiments with dpSVPs, a distinct type of subvirion particle that lacks σ3 but contains most molecules of μ1/μ1C still uncleaved at the δ-ϕ junction, provided support for this conclusion by showing that dpSVPs behave like ISVPs in a similar set of tested properties (15) (summarized in Table 2), despite the low level of δ-ϕ cleavage in dpSVPs. The analyses of rcISVPs here and of dpSVPs in the previous study (15) are thus consistent and complementary in demonstrating the key role of σ3 and the negligible role of δ-ϕ cleavage in determining the different particle behaviors.

Although we have clearly shown that σ3 affects the behavior of particles in several in vitro and in vivo assays, we have yet to define the molecular mechanisms by which σ3 exerts its effects. It appears likely that the presence of σ3 in particles inhibits one or more of the other capsid proteins from completing their function or functions in reovirus entry. Thus, when σ3 remains present after receptor binding and uptake by cells, as in infections with virions and rcISVPs, it must be cleaved by a cellular proteinase or proteinases to eliminate this inhibitory effect. Since activation to interact with membrane bilayers and to transcribe the viral mRNAs involves conformational changes in the outer capsid (8, 10, 14, 19, 22, 27, 30, 39), our current hypothesis is that σ3 acts primarily by limiting the conformational mobility of the relevant protein or proteins. Since σ3 has extensive interactions with μ1 in the virion outer capsid (21), and since μ1 has roles in membrane penetration and transcriptase activation, the effects of σ3 most likely occur through its interactions with μ1. Nonetheless, effects of σ3 on λ2 or σ1, the other two outer capsid proteins, are also conceivable. Po-

tential effects of σ3 on σ1 structure and functions in rcISVPs are a focus of current studies.

rcISVPs as reagents for mutational studies of σ3. The lack of an effective method for engineering mutations into the genomes of double-stranded RNA viruses in the family *Reoviridae* has hindered studies of various aspects of their biochemistry and biology. Our new method for recoating ISVPs, however, represents a simple yet effective system that can overcome this limitation in a partial way for the reovirus σ3 protein. By engineering selected mutations into an S4 cDNA clone, expressing mutant forms of recombinant σ3 protein, and using these mutant σ3 molecules to generate rcISVPs (29), we can now perform detailed characterizations of the effects of these mutations, both in vitro and in vivo, on the properties of σ3 relating to reovirus entry. A notable advantage of this system is that it does not rely on viral replication for recovery of infectious virions containing the mutant σ3 proteins. Thus, mutations that may have lethal effects on infection, and would be difficult or even impossible to amplify by using a more classical reverse-genetic approach, can be readily studied with our approach. The genetic analysis of σ3 cleavage rate included in this study provides a concrete demonstration of the utility of the recoating approach as a genetic tool and also demonstrates how chimeric proteins constructed to have different regions derived from different virus strains can be used in localizing the sequence determinants of strain-dependent differences in the behaviors of particle-bound proteins.

ACKNOWLEDGMENTS

We thank S. J. Harrison, J. J. Lugus, and X.-H. Zhou for excellent technical help and the other members of our laboratories for helpful discussions. We also thank K. Chandran, G. A. Manji, and S. A. Rice for insightful comments on preliminary versions of the manuscript.

This work was supported by NIH research grants AI-39533 (to M.L.N.), GM-33050 and AI-35212 (to T.S.B.), and AI-32139 (to L.A.S.); DARPA research contract MDA 972-97-1-0005 (to M.L.N.); research grants from the Lucille P. Markey Charitable Trust (to the Institute for Molecular Virology, University of Wisconsin—Madison, and the Structural Biology Center, Purdue University); NIH research technology grant RR-00570 (to the Integrated Microscopy Resource, University of Wisconsin—Madison); and American Cancer Society research grant RPG-98-12701-MBC (to L.A.S.). J.J.-V. was supported by a fellowship from La Caixa d'Estalvis i Pensions de Barcelona and by a Steenbock fellowship from the Department of Biochemistry, University of Wisconsin—Madison. M.L.N. received additional support as a Shaw Scientist from the Milwaukee Foundation. S.B.W. was supported by a Purdue Biophysics training grant and a Purdue Research Foundation fellowship.

REFERENCES

1. **Amerongen, H. M., G. A. R. Wilson, B. N. Fields, and M. R. Neutra.** 1994. Proteolytic processing of reovirus is required for adherence to intestinal M cells. J. Virol. **68:**8428–8432.
2. **Astell, C., S. C. Silverstein, D. H. Levin, and G. Acs.** 1972. Regulation of the reovirus RNA transcriptase by a viral capsomere protein. Virology **48:**648–654.
3. **Baer, G. S., and T. S. Dermody.** 1997. Mutations in reovirus outer-capsid protein σ3 selected during persistent infections of L cells confer resistance to protease inhibitor E64. J. Virol. **71:**4921–4928.
4. **Baker, T. S., and R. H. Cheng.** 1996. A model-based approach for determining orientations of biological macromolecules imaged by cryoelectron microscopy. J. Struct. Biol. **116:**120–130.
5. **Baker, T. S., J. Drak, and M. Bina.** 1988. Reconstruction of the three-dimensional structure of simian virus 40 and visualization of the chromatin core. Proc. Natl. Acad. Sci. USA **85:**422–426.
6. **Bodkin, D. K., M. L. Nibert, and B. N. Fields.** 1989. Proteolytic digestion of reovirus in the intestinal lumens of neonatal mice. J. Virol. **63:**4676–4681.
7. **Borsa, J., T. P. Copps, M. D. Sargent, D. G. Long, and J. D. Chapman.** 1973. New intermediate subviral particles in the in vitro uncoating of reovirus virions by chymotrypsin. J. Virol. **11:**552–564.
8. **Borsa, J., D. G. Long, T. P. Copps, M. D. Sargent, and J. D. Chapman.** 1974. Reovirus transcriptase activation in vitro: further studies on the facilitation phenomenon. Intervirology **3:**15–35.
9. **Borsa, J., B. D. Morash, M. D. Sargent, T. P. Copps, P. A. Lievaart, and J. G. Szekely.** 1979. Two modes of entry of reovirus particles into L cells. J. Gen. Virol. **45:**161–170.
10. **Borsa, J., M. D. Sargent, P. A. Lievaart, and T. P. Copps.** 1981. Reovirus: evidence for a second step in the intracellular uncoating and transcriptase activation process. Virology **111:**191–200.
11. **Borsa, J., M. D. Sargent, D. G. Long, and J. D. Chapman.** 1973. Extraordinary effects of specific monovalent cations on activation of reovirus transcriptase by chymotrypsin in vitro. J. Virol. **11:**207–217.
12. **Canning, W. M., and B. N. Fields.** 1983. Ammonium chloride prevents lytic growth of reovirus and helps to establish persistent infection in mouse L cells. Science **219:**987–988.
13. **Centonze, V. E., Y. Chen, T. F. Severson, G. G. Borisy, and M. L. Nibert.** 1995. Visualization of individual reovirus particles by low-temperature, high-resolution scanning microscopy. J. Struct. Biol. **115:**215–225.
14. **Chandran, K., D. L. Farsetta, and M. L. Nibert.** Unpublished data.
15. **Chandran, K., and M. L. Nibert.** 1998. Protease cleavage of reovirus capsid protein μ1/μ1C is blocked by alkyl sulfate detergents, yielding a new type of infectious subvirion particle. J. Virol. **72:**467–475.
16. **Chang, C.-T., and H. J. Zweerink.** 1971. Fate of parental reovirus in infected cell. Virology **46:**544–555.
17. **Coombs, K. M.** 1998. Stoichiometry of reovirus structural proteins in virus, ISVP, and core particles. Virology **243:**218–228.
18. **Cox, D. C., and W. Clinkscales.** 1976. Infectious reovirus subviral particles: virus replication, cellular cytopathology, and DNA synthesis. Virology **74:**259–261.
19. **Drayna, D., and B. N. Fields.** 1982. Activation and characterization of the reovirus transcriptase: genetic analysis. J. Virol. **41:**110–118.
20. **Drayna, D., and B. N. Fields.** 1982. Genetic studies on the mechanism of chemical and physical inactivation of reovirus. J. Gen. Virol. **63:**149–159.
21. **Dryden, K. A., G. Wang, M. Yeager, M. L. Nibert, K. M. Coombs, D. B. Furlong, B. N. Fields, and T. S. Baker.** 1993. Early steps in reovirus infection are associated with dramatic changes in supramolecular structure and protein conformation: analysis of virions and subviral particles by cryoelectron microscopy and image reconstruction. J. Cell Biol. **122:**1023–1041.
22. **Ewing, D. D., M. D. Sargent, and J. Borsa.** 1985. Switch-on of transcriptase function in reovirus: analysis of polypeptide changes using 2-D gels. Virology **144:**448–456.
23. **Fuller, S. D., S. J. Butcher, R. H. Cheng, and T. S. Baker.** 1996. Three-dimensional reconstruction of icosahedral particles—the uncommon line. J. Struct. Biol. **116:**45–55.
24. **Furlong, D. B., M. L. Nibert, and B. N. Fields.** 1988. Sigma 1 protein of mammalian reoviruses extends from the surfaces of viral particles. J. Virol. **62:**246–256.
25. **Gillian, A. L., and M. L. Nibert.** 1998. Amino terminus of reovirus nonstructural protein σNS is important for ssRNA binding and nucleoprotein complex formation. Virology **240:**1–11.
26. **Hayes, E. C., P. W. K. Lee, S. E. Miller, and W. K. Joklik.** 1981. The interaction of a series of hybridoma IgGs with reovirus particles. Demonstration that the core protein λ2 is exposed on the particle surface. Virology **108:**147–155.
27. **Hooper, J. W., and B. N. Fields.** 1996. Role of the μ1 protein in reovirus stability and capacity to cause chromium release from host cells. J. Virol. **70:**459–467.
28. **Jané-Valbuena, J., G. A. Manji, P. D. Friesen, and M. L. Nibert.** Unpublished data.
29. **Jané-Valbuena, J., S. Yue, L. A. Schiff, and M. L. Nibert.** Unpublished data.
30. **Joklik, W. K.** 1972. Studies on the effect of chymotrypsin on reovirions. Virology **49:**700–715.
31. **Kedl, R., S. Schmechel, and L. Schiff.** 1995. Comparative sequence analysis of the reovirus S4 genes from 13 serotype 1 and serotype 3 field isolates. J. Virol. **69:**552–559.
32. **Kothandaraman, S., M. C. Hebert, R. T. Raines, and M. L. Nibert.** 1998. No role for pepstatin A-sensitive proteinases in reovirus infections of L or MDCK cells. Virology **251:**264–272.
33. **Lee, P. W. K., E. C. Hayes, and W. K. Joklik.** 1981. Characterization of anti-reovirus immunoglobulins secreted by cloned hybridoma cell lines. Virology **108:**134–146.
34. **Lerch, R. A., and P. D. Friesen.** 1993. The 35-kilodalton protein gene (p35) of Autographa californica nuclear polyhedrosis virus and the neomycin resistance gene provide dominant selection of recombinant baculoviruses. Nucleic Acids Res. **21:**1753–1760.
35. **Lucia-Jandris, P., J. W. Hooper, and B. N. Fields.** 1993. Reovirus M2 gene is associated with chromium release from mouse L cells. J. Virol. **67:**5339–5345.
36. **Luongo, C. L., K. A. Dryden, D. L. Farsetta, R. L. Margraf, T. F. Severson, N. H. Olson, B. N. Fields, T. S. Baker, and M. L. Nibert.** 1997. Localization of a C-terminal region of λ2 protein in reovirus cores. J. Virol. **71:**8035–8040.
37. **Metcalf, P., M. Cyrklaff, and M. Adrian.** 1991. The three-dimensional struc-

ture of reovirus obtained by cryo-electron microscopy. EMBO J. **10:**3129–3136.
38. **Morgan, E. M., and H. J. Zweerink.** 1974. Reovirus morphogenesis. Corelike particles in cells infected at 39° with wild-type reovirus and temperature-sensitive mutants of groups B and G. Virology **59:**556–565.
39. **Nibert, M. L.** 1993. Structure and function of reovirus outer-capsid proteins as they relate to early steps in infection. Ph.D. thesis. Harvard University, Cambridge, Mass.
40. **Nibert, M. L., and B. N. Fields.** 1992. A carboxy-terminal fragment of protein μ1/μ1C is present in infectious subvirion particles of mammalian reoviruses and is proposed to have a role in penetration. J. Virol. **66:**6408–6418.
41. **Nibert, M. L., D. B. Furlong, and B. N. Fields.** 1991. Mechanisms of viral pathogenesis. Distinct forms of reoviruses and their roles during replication in cells and host. J. Clin. Investig. **88:**727–734.
42. **Nibert, M. L., L. A. Schiff, and B. N. Fields.** 1991. Mammalian reoviruses contain a myristoylated structural protein. J. Virol. **65:**1960–1967.
43. **Schmechel, S., M. Chute, P. Skinner, R. Anderson, and L. Schiff.** 1997. Preferential translation of reovirus mRNA by a σ3-dependent mechanism. Virology **232:**62–73.
44. **Severson, T. F., K. Chandran, A. L. Gillian, and M. L. Nibert.** Unpublished data.
45. **Shatkin, A. J., and A. J. LaFiandra.** 1972. Transcription by infectious subviral particles of reovirus. J. Virol. **10:**698–706.
46. **Shepard, D. A., J. G. Ehnstrom, and L. A. Schiff.** 1995. Association of reovirus outer capsid proteins σ3 and μ1 causes a conformational change that renders σ3 protease sensitive. J. Virol. **69:**8180–8184.
47. **Shing, M., and K. M. Coombs.** 1996. Assembly of the reovirus outer capsid requires μ1/σ3 interactions which are prevented by misfolded σ3 protein in temperature-sensitive mutant tsG453. Virus Res. **46:**19–29.
48. **Silverstein, S. C., M. Schonberg, D. H. Levin, and G. Acs.** 1970. The reovirus replicative cycle: conservation of parental RNA and protein. Proc. Natl. Acad. Sci. USA **67:**275–281.
49. **Strong, J. E., G. Leone, R. Duncan, R. K. Sharma, and P. W. K. Lee.** 1991. Biochemical and biophysical characterization of the reovirus cell attachment protein σ1: evidence that it is a homotrimer. Virology **184:**23–32.
50. **Sturzenbecker, L. J., M. Nibert, D. Furlong, and B. N. Fields.** 1987. Intracellular digestion of reovirus particles requires a low pH and is an essential step in the viral infectious cycle. J. Virol. **61:**2351–2361.
51. **Tillotson, L., and A. J. Shatkin.** 1992. Reovirus polypeptide σ3 and N-terminal myristoylation of polypeptide μ1 are required for site-specific cleavage to μ1C in transfected cells. J. Virol. **66:**2180–2186.
52. **Tosteson, M. T., M. L. Nibert, and B. N. Fields.** 1993. Ion channels induced in lipid bilayers by subvirion particles of the nonenveloped mammalian reoviruses. Proc. Natl. Acad. Sci. USA **90:**10549–10552.
53. **Virgin, H. W., IV, M. A. Mann, B. N. Fields, and K. L. Tyler.** 1991. Monoclonal antibodies to reovirus reveal structure/function relationships between capsid proteins and genetics of susceptibility to antibody action. J. Virol. **65:**6772–6781.
54. **Walker, S. B., K. Chandran, M. L. Nibert, and T. S. Baker.** Unpublished data.
55. **Wetzel, J. D., G. J. Wilson, G. S. Baer, L. R. Dunnigan, J. P. Wright, D. S. H. Tang, and T. S. Dermody.** 1997. Reovirus variants selected during persistent infections of L cells contain mutations in the viral S1 and S4 genes and are altered in viral disassembly. J. Virol. **71:**1362–1369.
56. **Yue, Z., and A. J. Shatkin.** 1996. Regulated, stable expression and nuclear presence of reovirus double-stranded RNA-binding protein σ3 in HeLa cells. J. Virol. **70:**3497–3501.